To mow or not to mow: reed biofilms as denitrification hotspots in drainage canals

Elisa Soana*, Anna Gavioli, Elena Tamburini, Elisa Anna Fano, Giuseppe Castaldelli

Department of Life Sciences and Biotechnology, University of Ferrara, Via L. Borsari 46 - 44121 Ferrara – Italy

*Corresponding author: elisa.soana@unife.it

Abstract

In shallow-water systems with calm hydrodynamic, dense vegetation stands provide most of the available surface for periphyton development. The large ratio between biological active surfaces and water volume amplifies the influence of biofilm activity on water chemistry, resulting the key factor responsible for nitrogen removal performance of wetlands and waterways. However, the denitrification capacity of biofilms on emergent macrophytes remains understudied, especially if investigated on dead stems during the non-vegetative season.

The aims of the present study were: 1) to quantify the role of biofilms colonizing dead stems of *Phragmites australis* in NO_3^- mitigation via denitrification in winter (~11°C) in a NO_3^--rich drainage canal; 2) to determine how the biofilm denitrifying capacity varies as a function of water velocity (0-6 cm s^{-1}). Denitrification was assessed by the concomitant measurements of NO_3^- consumption and N_2 production from analyses of N_2:Ar by Membrane Inlet Mass Spectrometry.

Sediments with biofilms were found more efficient in converting NO_3^- to N_2 (7-17 mmol N m^{-2} d^{-1}) than bare sediments (3-5 mmol N m^{-2} d^{-1}). Denitrification activity in biofilms responded positively to increasing water velocity that enhanced the rate of NO_3^- supply to the biologically active surfaces.

Results of the present study highlighted that denitrification performed by biofilms on senescent stems proceeds beyond the vegetative season throughout the cold period and maintains the depuration capacity when drainage ditches may still drive high NO_3^- loads leached from the agricultural fields. This highlights the important role of a diversified and extended microbial community. Together with water velocity these features should be taken into account as key elements in the management of the hydrographic network aimed at combining hydrological needs and water quality goals.

Keywords

Biofilms, nitrate removal, denitrification, N_2 open-channel method, water velocity, canal network

1. Introduction

Nitrogen (N) cycling in shallow aquatic environments is strongly regulated by the interactions between microbial communities and aquatic plants. It has commonly been observed that sediments colonised by emergent macrophytes mitigate nitrate (NO_3^-) loads more effectively than unvegetated ones, improving the N removal performances of natural and artificial aquatic ecosystems (Weisner et al., 1994; Faulwetter et al., 2009; Soana et al., 2017). Macrophytes control inorganic N availability both directly, by assimilation, and indirectly by affecting the coupling among ammonification, nitrification and denitrification, mainly due to oxygen injection into the rhizosphere via the aerenchyma and exudation of organic carbon from roots (Vila-Costa et al., 2016; Rehman et al., 2017). Aquatic plants may also drive N dynamics because submersed portions like stems and leaves provide large amounts of additional surfaces for the growth of periphyton, considered hot spots of N transformations (Toet et al., 2003; Pang et al., 2016). Periphyton (also "biofilms") is an ubiquitous complex matrix of living (algae, bacteria, and other micro-organisms, such as fungi and protozoa) and non-living components (organic detritus, deposited fine sediments, polymeric substances secreted to hold the biofilm together) attached to various submerged substrates in the photic zones of aquatic ecosystems (Wetzel, 1983; Roeselers et al., 2008). Referred as epiphyton when colonizing plant tissues, it is an ensemble of autotrophs and heterotrophs whose synergic metabolism results in the estabilishment of proximate oxic and anoxic micro-niches enabling the co-occurrence of contrasting redox processes at a small spatial scale, e.g. coupled nitrification/denitrification (Eriksson, 2001; Revsbech et al., 2005; Zhang et al., 2016).

Due to limited oxygen penetration, the benthic compartment is commonly considered the elective site for denitrification. However, a number of researchers have shown that biofilms attached to submersed plant surfaces, although highly variable in species composition and coverage, may sustain denitrification activity with rates comparable or even higher than in sediments, making a significant contribution to overall NO_3^- removal at the ecosystem level in nutrient-rich environments. Eriksson and Weisner (1997) demonstrated that also old stems of submersed plants

were sites as active as sediment for denitrification in a eutrophic wetland, due to leakage of nutrients from the senescent tissues and a shift from a autotrophic to a heterotrophic-dominated biofilm as it aged. Similarly, Toet and collaborators (2003) reported that on a daily basis the main contribution to the NO_3^- removal capacity of a wetland during winter was ascribed to biofilms on old stems of *Phragmites australis* that maintained denitrification rates comparable to those measured in periods with more favourable temperatures. Although rates are usually strongly affected by the intertwined action of several chemico-physical and biological drivers (e.g. nutrient level, hydraulic conditions, redox status, abundance of vegetation, periphyton biomass), the key elements promoting the biofilm denitrifying activity seem to be the supply of NO_3^- from the water column and of labile organic carbon produced by the periphytic algae, with a weak effect of temperature (Toet et al, 2003; Srivastava et al., 2017).

NO_3^- removal rates faster than diffusion from the surrounding waters may represent an important constraint for denitrification. Laboratory experiments aimed at investigating how variable velocities affect denitrification in benthic and epiphytic biofilms revealed that the process is regulated by the complex interplay between the transport of NO_3^- to anoxic niches and the overall redox status of the biological layers mediated by the water flow (Eriksson, 2001; Arnon et al., 2007a). Increasing velocity tends to enhance denitrification rates by the action of continuous mixing of NO_3^--poor water layers around uptake surfaces and overlying NO_3^--rich water, a condition that ensures a constant supply to the microbial community (Sirivedhin and Gray, 2006). However, being facultative anaerobes, denitrifiers shift to aerobic metabolism when oxygen is available, thus denitrification may be suppressed when biofilms become well flushed with oxygen as a conseguence of high hydrodynamic conditions (Arnon et al., 2007b; O'Connor and Hondzo, 2007).

In shallow-water systems with calm hydrodynamic, macrophytes generally provide most of the accessible surface for periphyton development, leading to a large ratio between the biologically active surfaces and the water volume and amplifying the influence of biofilm activity on water chemistry (Wetzel and Søndergaard, 1998). Although epiphytic biofilms are usually implied in the

majority of organic matter processing and biogeochemical cycles, and they are thus responsible of the nutrient removal performance of wetlands and waterways, very few studies have provided quantitative estimations of the denitrification capacity in periphyton on emergent plants (Toet et al; 2003; Venterink et al., 2003; Yamamoto et al., 2005). In almost the totality of the cases, the process was evaluated in terms of potential rates obtained in non limitig conditions, whose extrapolation up to the ecosystem-level is usually tricky and not reflecting the actual in field rates. The relationship between water velocity and denitrification has been scarcely investigated in biofilms on submerged macrophytes (Eriksson, 2001), and no studies are available for biofilms on emergent plants performed in intact freshwater sediments by the simultaneous measurements of NO_3^- consumption and N_2 production. Furthermore, very little attention has been paid to evaluate if NO_3^- mitigation by periplyton on dead stems of emergent vegetation is maintained also during the non-vegetative season when large loads of nutrients are carried by rivers and canals in agricultural landscapes.

The aims of the present study were: 1) to quantify the role of biofilms colonizing dead stems of *Phragmites australis* in NO_3^- dissipation via denitrification during winter season in a drainage canal affected by non-point source pollution; 2) to determine if biofilm denitrifying capacity varies as a function of water velocity. N removal was quantified in laboratory mesocosms simulating slow-flow waterways by the simultaneous measurement of N_2 production (N_2:Ar open-channel method) and NO_3^- consumption. Three velocities (1.5, 3, and 6 cm s^{-1}) and the condition with no flow were set to cover the typical range of flow variation in canals and ditches of lowland agricultural basins.

By working in nature, it is generally extremely difficult to isolate the effect of a single variable (e.g. water velocity) on denitrification, since other important regulating factors, such as NO_3^- concentration and water temperature, may vary at the same time. The mesocosm experimental design represents a reproducible alternative to *in situ* studies where elements of variability of the canal stretches are eliminated and the tested variable may be systematically manipulated.

2. Material and Methods

2.1 Mesocosm construction and pre-incubation procedure

Mesocosms were built using water, bare sediment and sediment with dead stems of *P. australis* colonized by periphyton, sampled in winter in a slow-flow (< 10 cm s^{-1}) canal (44°48'53.17"N; 11°43'23.14"E) where denitrification and NO_3^- removal rates were previously measured by N_2:Ar and N mass balance methods (Castaldelli et al., 2015). The study site belongs to the Po di Volano basin (~2,600 km^2, Northern Italy) an intensively cropped deltaic territory characterized by a flat topography and an extensive network of drainage and irrigation ditches. Here, natural propagation and seasonal evolution of aquatic vegetation are strongly affected by yearly maintenance operations aimed at preserving hydraulic performance. Thus, stands of common reed (*Phragmites australis* Cav. Trin. ex Steud), cattail (*Typha latifolia* L.) and great manna grass (*Glyceria maxima* Hartm. Holmb.), usually monospecific, are maintained only in rare isolated stretches.

Mesocosms were designed to simulate vegetated waterways or wetlands with moving water and built as follows (Fig. 1): an external Plexiglass tube with internal diameter of 29 cm and an internal tube with external diameter of 12 cm were positioned concentrically on a Plexiglass circular base, to define an annulus of total surface 547 cm^2 (annular radius width 8.5 cm). Parcel of sediments were sampled using a steel shovel with finely sharpen edge and placed in the chambers to define a continuous annulus of sediment having a height of maximum 25 cm when including the rhizosphere. The used mesocosm dimension was compatible for establishing a homogeneous water flow inside each chamber without sediment resuspension, and, not less important, it allowed an operatively viable hand collection of the sediment by maintaining intact the rhizosphere without damaging the *P. australis* rhizomes. Three chambers with sediment and dead stems of *P. australis* (18-30 plants in each mesocosm, 1300-2200 g of above-ground dry biomass per m^2) and three chambers only with sediment were developed. In an hour after collection, they were transferred from the field to an outdoor, non-shaded area at the Department of Life Sciences and Biotechnology, University of Ferrara, and maintained under natural weather conditions. Here, the

chambers were placed in two separate cylindrical tanks (87 cm diameter and 105 cm high polyethylene containers), one for vegetated replicates and one for replicates devoid of vegetation. The chambers were gently flooded with canal water maintained recirculated and exchanged between the chambers and the tanks by aquarium pumps. Water level in the tanks was controlled every day and water from the canal was added to compensate for evapotranspiration loss. The chambers were maintained fully submerged in canal water and they were allowed to equilibrate for some weeks before the incubations. Each tank was connected with a thermostat to maintain temperature constant at 11°C during pre-incubation and incubation procedures. Pre-incubation and incubation procedures were performed according to standard protocols (Dalsgaard et al., 2000).

2.2 Incubation procedure

Each chamber was equipped with 12-V low flow submersible pump (Whale®) connected to a multichannel electronic rheostat with a voltage regulation. Each pump was submerged at 4 cm below the water surface to prevent bubbling. A plastic tube connected to the pump was placed vertically in the water column and oriented in a way to create a constant and homogeneous flow within the chamber without sediment resuspension (Fig. 1). Voltage level was regulated in each chamber to yield an average flow velocity of 0, 1.5, 3, and 6 cm s^{-1}, checked with a current meter, vertically and on the middle of the annular radius and in the middle of the water column.

Incubations were performed in four consecutive days of late winter (from 02.28.2017 to 03.03.2017) during stable meteorological conditions. A different velocity was applied each day in the mesocosms, from 0 to 6 cm s^{-1}, and they were incubated in the dark and in the light to discriminate the effect of photosynthetic processes on N retention. Average air temperature was 8.9±3.3°C and 14.2±3.1°C during incubations performed in dark and light conditions, respectively. Solar radiation during light phase averaged 423±209 W m^{-2} (University of Ferrara weather station).

Before any incubation, the water in each of the two tanks was replaced with water sampled during the previous day from the canal to avoid nutrient deficiency. Ammonium and nitrite concentrations

were always below detection limits. NO_3^- concentration was standardized to 100 µM at the time zero of each incubation by adding an appropriate volume of a stock NO_3^- solution (200 mM KNO_3). The value of 100 µM was chosen because it approximates the typical average NO_3^- availability in ditches and canals of the investigated area, affected mainly by non-point source pollution and where ammonium and nitrite are constantly below detection limits (Pierobon et al., 2013; Castaldelli et al., 2015). Water temperature and NO_3^- availability were maintained as similar as possible among incubations, and the only variables that were varied and that hence affected N removal process were water velocity and light conditions.

Incubations started when the water level in the tanks was lowered below the chamber tops and each mesocosms was isolated. Oxygen concentrations were in the range 250-300 µM, and during the incubation time they never changed by more than ±20% of the initial value. Water samples were collected using a glass syringe from the mid-depth of each mesocosms at regular time intervals to follow the temporal evolution of NO_3^- and N_2. At each sampling, water temperature and conductivity were also measured with a multiparametric probe. Samples for NO_3^- determinations were filtered through Whatman GF/F glass fiber filters, and transferred to polyethylene vials. NO_3^- was measured on a Technicon AutoAnalyser II (Armstrong et al., 1967; detection limit 0.4 µM; precision ±5%). Samples for N_2:Ar determinations were transferred into 12-ml gastight glass vials (Exetainer®, Labco, High Wycombe, UK), flushing at least 3 times the vial volume and preserved by adding 100 µl of 7M $ZnCl_2$ solution. The N_2:Ar ratio in water samples was measured within one week at the laboratory of Aquatic Ecology, University of Ferrara, by MIMS (Bay Instruments, USA; Kana et al., 1994), a PrismaPlus quadrupole mass spectrometer with an inline furnace operating at 600°C to allow for O_2 removal. The coefficient of variation calculated from replicated N_2:Ar samples (n=10) was 10-fold lower (~0.04%) than N_2 measurements, similarly to Laursen and Seitzinger (2002). N_2 concentration was calculated from the measured N_2:Ar multiplied by the theoretical saturated Ar concentration at the sampling water temperature, which was determined from gas solubility tables (Weiss, 1970).

Additional samples for N_2O determinations were collected in the same way of those for N_2:Ar and analysed by gas chromatography (Trace GC, 2000 Series, Thermo Finnigan, San Jose, CA, USA equipped with an ECD detector). N_2O production resulted negligible as previous experiments demonstrated both at the reach-scale and in laboratory mesocosms (Castaldelli et el., 2015).

2.3 Biofilm characterization

At the end of all incubations, the density of *P. australis* stems, the diameter of each stem, and the height of submerged portion were measured in each vegetated mesocosm for the estimation of the total surface available for biofilm colonization. For biofilm characterization, the dead stems were first cut at the water surface, then the submerged portions were removed just above the sediment. The entire biofilm was gently scraped off with a toothbrush from the surface, and homogenized in synthetic freshwater at the average conductivity and pH of the water used for the incubations. On three aliquots of the homogenized suspension, chlorophyll-*a* content was determined spectrophotometrically after extraction with 90% acetone (Lorenzen, 1967). The remaining suspension was dried at 50°C for 36 hours, weighed for determination of the total dry mass of the biofilm, and finally expressed in term of dry weight per m^2 of colonised reed surface (g DW m^{-2}). This procedure was repeated separately for each mesocosm. Chlorophyll-*a* content was used as a proxy of the proportion of autotrophic community of biofilm (Kiss et al., 2003).

2.4 Calculation of NO_3^- removal and N_2 production rates

Hourly rate of NO_3^- removal (µmol N m^{-2} h^{-1}) was calculated for each mesocosm from the rate of change in concentrations with time and expressed as per m^2 of sediment. The water volume collected for analysis was overall <2% of the total volume included in each chamber; anyway, a correction factor was considered to account for the loss of water volume from the subsequent samplings.

Net N_2 fluxes at the mesocosm scale (μmol N m^{-2} h^{-1}) were calculated by modelling the conversion of NO_3^- into N_2 with the simultaneous air-water exchange, similarly to the estimation of reach-scale denitrification proposed by Laursen and Seitzinger (2002). The general assumption is that in an open-top chamber, where water flow is artificially set, N_2 concentrations evolve temporally due to metabolic activity and as a function of temperature that affects the gas exchange between water and atmosphere, similarly to a Lagrangian transport in a natural watercourse. The constant temperature conditions maintained by thermostats in the tanks allowed the stability of the gas fluxes across the water-atmosphere interface during the course of the experiments. This approach determines net N_2 fluxes because the measured N_2 concentrations are the results of production (i.e. denitrification including coupled nitrification/denitrification, anammox -anaerobic ammonium oxidation) and consumption (i.e. N fixation) processes. However, the terms "denitrification" and "N_2 production" (or N_2 flux) are used interchangeably in the text, since the contribution of anammox is usually low in eutrophic freshwater environments (Zhou et al., 2014; Shen et al., 2016).

Net N_2 fluxes for each mesocosm were simulated at 1-min time steps using the following model input parameters (Laursen and Seitzinger, 2002): measured N_2 and water temperature at each sampling time, average water velocity set in the mesocosm, dimension of the moving parcel (water column height × annular radius), gas transfer velocity (k600), and Schmidt number coefficient (−2/3 typical for water surfaces without waves, Jähne et al., 1987). The reaeration coefficient of oxygen at 20°C (KO_2, 20°C, d^{-1}) was calculated from flow velocity u (m s^{-1}) and water depth d (m) by the general empirical equation by Genereux and Hemond (1992):

$$K_{O_2} = a \cdot \frac{u^b}{d^c}$$

The parameters of *a*, *b*, and *c* were taken by the literature where measurements of gas transfer in re-circulating cylindrical flumes were performed within velocity-depth ranges comparable to that adopted in the present study (Isaacs and Gaudy, 1968; Eloubaldy, 1969; Isaac et al., 1969; Negulescu and Rojanki, 1969; Padden and Gloyna, 1972). These equations were tested and applied in laminar flow channels, artificial flumes, and regular-shaped sewers (Cox, 2003), and generally

identified as the most reliable choice in review studies about reaeration equations (Palumbo and Brown, 2013). The transfer velocity of oxygen (kO_2, 20°C, cm h^{-1}) was calculated by multiplying the average value of O_2 reaeration coefficient, obtained by applying the aforementioned set of equations, by the average water column depth of each mesocosm, assuming a well-mixed water column. The gas transfer velocity was finally normalized to a Schmidt number of 600 (k600, for CO_2 at 20 °C, cm h^{-1}) (Jähne et al., 1987; Wanninkhof, 1992).

The general equation of Genereux and Hemond (1992) for calculating the O_2 reaeration coefficient cannot be used in stagnant waters. Moreover, when wind speed is almost null as generally occurs in the lower Po valley, neither wind-based models are suitable (Cole and Caraco, 1998). Under stagnant conditions, gas exchange is low but not null. Thus with a conservative approach, we adopted the lower extreme of the k600 range obtained for the lowest velocity level (1.5 cm s^{-1}) with the above reported depth-velocity equations.

The approach adopted to estimate the net N_2 fluxes cannot be used in stagnant conditions since a Lagrangian transport of the water parcel (at the reach scale or at the mesocosm scale) is required. N_2 production rate was calculated for each mesocosm from the rate of change in concentrations with time and expressed as per m^2 of sediment, corrected for the N_2 efflux from the water column to the atmosphere (Jacobs and Harrison, 2014), as N_2 concentrations were constantly higher than the theoretical saturated N_2 concentration at the sampling water temperature. This procedure assumes the N_2 concentrations in the mesocosm water column were at steady state. The efflux was calculated as the product of the difference between the measured N_2 concentration in the water column and the theoretical saturated N_2 concentration at the sampling water temperature determined from gas solubility tables (Weiss, 1970), and the N_2 reaeration coefficient. The estimates of KO_2 were converted to KN_2 based on the respective Schmidt numbers of this gas calculated for water temperature at the sampling times, according to the polynomial fit given by Wanninkhof (1992).

To discriminate the effect of biofilm alone and allow comparisons with the literature, hourly N fluxes measured in mesocosms with sediment and biofilm were corrected for values measured in

mesocosms with only sediment for each tested condition, and normalized for the surface suitable for biofilm colonization (i.e. *P. australis* submerged stems). A similar benthic activity was assumed in the two mesocosm types, given the low incubation temperature and the plant dormancy phase resulting in its null direct effects on sediment dynamics. Due to slow degradation rates, dead stems were almost completely intact and in a standing position when the mesocosms were sampled and incubated. Senescent falling leaves were removed to avoid difference in the supply of organic matter to the sediment in the two mesocosm types.

Hourly rates of NO_3^- removal and denitrification were multiplied by the average number of light (11) and dark (13) hours in the winter period of the investigated area (Allen et al., 1998) and summed to obtain daily values (mmol N m^{-2} d^{-1}).

2.5 Statistical analyses

The effect of factors *velocity*, and *light condition* (light/dark) on hourly NO_3^- removal and N_2 production rates was tested by a two-way analysis of variance (ANOVA), separately for data from bare mesocosms and from mesocosms with biofilms to exclude any predictable significance due to the presence of epiphytes (Toet et al., 2003). Two-way ANOVA was also used to test the effect of factor *biofilm presence* and *velocity* on daily NO_3^- removal and N_2 production rates. Significant differences among velocity levels was identified by Holm-Sidak multiple comparison test. Normality (Shapiro–Wilk test) and homoscedasticity (Levene's test) were previously examined. Sample size was equal in all tests and all datasets fulfilled the requirements for parametric analyses. Linear regression analysis was performed to relate NO_3^- removal and N_2 production rates. Statistical significance was set at $p \leq 0.05$. Statistical analyses were performed with SigmaPlot 11.0 (Systat Software, Inc., CA, USA). Graphs and tables report average values with associated standard deviation (std. dev.).

3. Results

297 *3.1 Incubation conditions and biofilm characterization*

298 Initial mesocosm conditions were very similar among the different incubations performed at the
299 three velocities and with stagnant water (Table 1). Water temperature varied between 10.40°C and
300 11.59°C, and between 10.22 and 11.35°C, for dark and light incubations, respectively, and
301 conductivity was on average 590 µS cm^{-1}. After KNO_3 stock solution addition, mean NO_3^-
302 concentration in the mesocosm water column was increased up to 95-103 µM. k600 values
303 predicted as a function of water velocity and depth were in the range 0.45-0.99, 0.88-1.69, and 1.81-
304 3.00 cm h^{-1}, for 1.5, 3, and 6 cm s^{-1} velocity condition, respectively (Table 1). Minimum values
305 were obtained by applying the equation proposed by Isaacs et al. (1969), while maximum values
306 resulted from the parameterizations by Padden and Gloyna (1972) and Negulescu and Rojanki
307 (1969).

308 The submerged reed surface available for biofilm colonization was equal on average to 2.4 times
309 the sediment area of the mesocosm (range 1.6-2.8 m^{-2} m^{-2}). Biomass of the biofilm attached to the
310 submerged stems of dead *P. australis* averaged 10-12 g DW per m^2 of colonised surface,
311 representing a small mass (<20 g DW m^{-2}) according to a classification system of reed-epiphyton
312 developed for shallow slow-flow environments (Kiss et al., 2003). Chlorophyll-*a* content averaged
313 9-15 mg m^{-2} that expressed as percentage of dry biomass (<0.1%) allowed to characterize the
314 biofilm as heterotrophic, according to the previously mentioned classification.

315

316 *3.2 N fluxes in dark and light across the velocity range*

317 Mesocosms with biofilms colonizing dead stems of *P. australis* were always a greater NO_3^- sink
318 and N_2 source than mesocosms with bare sediment in all the tested conditions (Table 2, Fig. 2).
319 Across the velocity range, NO_3^- removal varied between 204±29 (stagnant condition, light) and
320 541±279 µmol N m^{-2} h^{-1} (6 cm s^{-1} velocity, dark) in presence of biofilms, and between 58±48 (1.5
321 cm s^{-1} velocity, light) and 178±38 µmol N m^{-2} h^{-1} (6 cm s^{-1} velocity, dark) in bare sediments (Fig.

2). NO_3^- removal rates were significantly higher in dark than in light conditions, both in presence and absence of biofilms (Table 2).

Water velocity had a significant but complex effect on NO_3^- dissipation. For mesocosms with biofilms, NO_3^- consumption across the velocity range followed two distinct patterns in the dark and in the light. In the dark, NO_3^- removal rates increased steadily in flowing conditions (+70%), when velocity increased from 1.5 cm s^{-1} to 6 cm s^{-1}, with the highest rate measured at 6 cm s^{-1} (Table 3), but in stagnant conditions the rates were higher (+37%) than at the first velocity level, i.e. 1.5 cm s^{-1}. Otherwise, in the light, NO_3^- removal rates increased steadily (+116%), when the velocity increased from 0 to 6 cm s^{-1}. In bare sediments, NO_3^- removal rates were not significantly different among different velocities (Table 2).

Across the velocity range, N_2 production ranged between 209±83 (1.5 cm s^{-1}, light) and 803±280 µmol N m^{-2} h^{-1} (6 cm s^{-1}, dark) in presence of biofilms, and between 90±45 (stagnant condition, light) and 233±14 µmol N m^{-2} h^{-1} (1.5 cm s^{-1} velocity, dark) in bare sediments (Fig. 2). In presence of biofilms, N_2 production rates were significantly higher in the dark than in the light and significantly different among velocities (Table 2). The pattern of N_2 fluxes across the velocity range was similar to that observed for dark NO_3^- removal, i.e. the highest rate was measured at 6 cm s^{-1} (Table 3), and the rates for the other flowing conditions (1.5 and 3 cm s^{-1}) were lower than the stagnant control condition. N_2 production was enhanced on average by 127% and by 196% in the dark and in the light, respectively, when velocity increased from 1.5 cm s^{-1} to 6 cm s^{-1}. The maximum difference between dark and light rates (both NO_3^- consumption and N_2 production) of the same velocity level was detected in stagnant conditions. In absence of biofilms, N_2 production rates measured in stagnant condition tended to be on average lower than rates measured in all the other flowing conditions, but not significantly different between light and dark and among velocity levels (Table 2).

3.3. Contribution of biofilms to overall NO_3^- removal and N_2 production in P. australis stands

348 Across the velocity range, rates of NO_3^- removal and N_2 production ascribed to biofilms alone
349 (expressed per m^2 of colonised reed surface) varied between 59±15 (stagnant condition, light) and
350 158±45 µmol N m^{-2} h^{-1} (6 cm s^{-1}, dark), and between 63±21 (1.5 cm s^{-1}, light) and 292±74 µmol N
351 m^{-2} h^{-1} (6 cm s^{-1}, dark), respectively (Fig. 3). The factor velocity was highly significant for both
352 NO_3^- removal and N_2 production (Table 2).
353 Dark N_2 production, light N_2 production and dark NO_3^- consumption in biofilms showed similar
354 patterns across the velocity range, i.e. the highest rate was measured at 6 cm s^{-1} (Fig. 3), and the
355 rates for the other flowing conditions (1.5 and 3 cm s^{-1}) were lower than the stagnant control
356 condition. Only light NO_3^- consumption raised constantly with increasing velocity. The rise in
357 velocity from 1.5 cm s^{-1} to 6 cm s^{-1} determined an enhancement of over 90% in daily NO_3^-
358 consumption, and the increase was even more considerable for daily N_2 production (+210%) (Fig.
359 3).
360 Daily NO_3^- consumption was significantly higher in reed stands with biofilms than in bare
361 sediments (p<0.001), with rates ranging between 7±1 and 12±3 mmol N m^{-2} d^{-1}, and between 2±1
362 and 4±1 mmol N m^{-2} d^{-1}, respectively (Fig. 4). NO_3^- removal rates were significantly different
363 among velocity levels only in mesocosms with biofilms (p<0.05). Daily NO_3^- removal remained < 9
364 mmol N m^{-2} d^{-1} when velocity varied between 0 and 3 cm s^{-1}, with an increase up to 12 mmol N m^{-2}
365 d^{-1} at 6 cm s^{-1}. For a unit of reed stand area, the major contribution to overall NO_3^- removal (57-
366 74%) was always ascribed to biofilms on dead stems (Fig. 4).
367 Similarly to NO_3^- consumption, daily N_2 production was significantly higher in presence of biofilms
368 than in absence (p<0.001). Daily N_2 production rates varied across the velocity range between 7±1
369 and 17±2 mmol N m^{-2} d^{-1} in mesocosms with dead stems of *P. australis* and biofilms, and between
370 3±1 and 5±1 mmol N m^{-2} d^{-1} in bare sediments (Fig. 4). Velocity had a significant effect on daily N_2
371 fluxes in mesocosms with biofilms (p<0.001). The highest rate was detected at 6 cm s^{-1} (Fig. 4),
372 while the rates at the other flowing conditions (1.5 and 3 cm s^{-1}) were lower than the stagnant
373 control condition. With velocity increasing from 1.5 cm s^{-1} to 6 cm s^{-1}, N_2 production increased by

more than 70%. For a unit of reed stand area, biofilms on dead stems was the main substratum to overall N_2 production (56-70%), with the only exception of the lowest velocity level (Fig. 4). Daily rates of NO_3^- removal and denitrification were significantly correlated (R^2=0.84, p<0.0001, n=24) (Fig. 5).

4. Discussion

4.1 Velocity as a key factor regulating denitrification in biofilms on emergent vegetation

The present study contributes to the understanding of denitrification performance, under varying water velocity, of biofilms colonizing dead stems of *P. australis* in agricultural drainage canals during winter season. Our results demonstrated that one square meter of canal bottom with dead reed stems contributes two to three times more to in-stream NO_3^- removal than one devoid of vegetation due to enhanced surfaces. The general good agreement between NO_3^- consumption and N_2 production suggests that denitrification of water column NO_3^- was the dominating mechanism driving N dissipation. Uptake of water column NO_3^- by periphytic microorganisms was not estimated in the present study but similar cases reported its negligible contribution to the overall NO_3^- removal (Kreiling et al., 2011; Messer et al., 2017).

The velocity as a key factor regulating N removal in eutrophic aquatic ecosystems remains poorly explored, generally limited to experiments performed on laboratory cultivated periphyton (Arnon et al., 2007a; O'Connor and Hondzo, 2007), and to some in field evidences not further adequately investigated, such as the greater NO_3^- removal capacity of constructed wetlands in well-mixed compared to stagnant conditions (Sirivedhin and Gray, 2006; Kjellin et al., 2007). In the present study, performed at winter temperatures for Northern Italy (~11°C), denitrification activity in epiphytic biofilms on dead stems of *P. australis* responded positively to increasing water flow velocity, even within the low range of velocities employed in the mesocosms to simulate those commonly found in agricultural ditches and canals of the investigated watershed. When velocity increased from the lowest (1.5 cm s^{-1}) to the highest (6 cm s^{-1}) level, daily rates of NO_3^- removal

400 almost doubled and daily rates of N_2 production more than tripled. Hydrodynamic characteristics of
401 the flowing water control the fluxes of nutrients and gas between the water and the biofilms,
402 regulating their metabolic activity. Under slow-flow conditions, NO_3^- supply to anoxic zones where
403 denitrification occurs may be limiting because as the water movement increases the thickness of the
404 diffusive boundary layer decreases, enhancing the transport of NO_3^- deeper into the biofilm
405 (Silvester and Sleigh 1985). The stimulating effect of NO_3^- availability on denitrification was
406 previously observed in biofilms on submerged macrophytes (Eriksson and Weisner, 1996), with
407 higher rates at sites with a constantly higher nutrient input than at nutrient-depleted sites in
408 conditions of similar periphytic biomass.
409 In the dark, a similar pattern across the entire velocity range was detected both for N_2 production
410 and NO_3^- consumption, i.e. the highest rates were measured at the highest velocity but the rates at
411 1.5 and 3 cm s^{-1} were lower than the control in stagnant conditions. Similar outcomes were found
412 by Eriksson (2001) that investigated the effect of water velocity on denitrification in periphyton
413 mats associated with submersed vegetation. In that study, the highest rates measured in stagnant
414 water were ascribed to the removal of the inhibitory effect of oxygen on denitrification. In absence
415 of running water, high respiration rates of dense meadows of submersed vegetation and associated
416 epiphytic community and limited diffusion may induce low oxygen concentrations around biofilms
417 not compensated by the renewal with oxygen-rich water, especially during the night, promoting the
418 establishment of diffuse niches suitable to NO_3^- dissipation via denitrification (Eriksson, 2001).
419 Similarly, in our mesocosms, high oxygen consumption rates by degradation processes and
420 heterotrophic activity may have favoured the creation of conditions suitable for denitrification.
421 However, in general, the rates measured in stagnant conditions are representative values only if
422 considered in a short term of few hours or less, until NO_3^- availability is not limited by the diffusion
423 from the water column to the biofilm active surfaces. After that, when NO_3^- supply is depressed by
424 the absence of water exchanges, denitrification eventually stops and, at low oxygen levels, not even
425 nitrification can fuel denitrification.

For the highest velocity adopted, N_2 fluxes measured in presence of biofilms were on average greater than the corresponding NO_3^- fluxes both in dark and light conditions. The contribution of nitrification in producing NO_3^- from mineralized ammonium in the aerobic layers of biofilms, subsequently denitrified to N_2 in the anaerobic layers, cannot be excluded, even if not directly quantified in the present study. Indeed, higher hydrodynamic transport as a consequence of higher velocity may have increased not only the supply of NO_3^- but also the delivery of oxygen to bioactive surfaces, making then sufficiently aerobic to provide ideal sites for processes such as aerobic degradation and nitrification, while maintaining at the same time favourable conditions for denitrification to occur, likely in the deeper biofilm layers. Efficient nitrification of mineralized NH_4^+ may have fuel denitrification by producing an additional NO_3^- source. N_2 production without any concomitant net NH_4^+ release suggests that the N cycle reactions, i.e. ammonification, nitrification and denitrification, were tightly coupled in space and time, as previously demonstrated for submersed vegetation stands in shallow aquatic environments (Eriksson and Weisner, 1999; Eriksson, 2001).

4.2 Effect of dark and light conditions on denitrification activity

Biofilms can support denitrification even when oxygen concentration in the surrounding water is considerably higher than the suboxic conditions (<0.2 mg O_2 l^{-1}), generally considered the threshold for denitrification to occur. This happens because, similarly to the benthic compartment, thick biofilms may exhibit a strong redox stratification, as a result of the balance between O_2 producing and consuming processes, thus denitrification may take place in the anoxic deeper layers, although oxygen availability in the water column remains high. N_2 production and NO_3^- consumption in biofilms on dead stems of *P. australis* were systematically higher in the dark than in the light along the whole velocity range established in the mesocosms. Even if not directly measured in the present study, we speculate that the diurnal redox fluctuations across biofilms were likely the major factor responsible for the diurnal changes of denitrification rates, as previously demonstrated for other

452 eutrophic environments (Sørensen et al., 1988; Christensen et al., 1990). Indeed, as denitrifiers are
453 facultative anaerobic bacteria, their activity is generally inhibited by the photosynthesis of the
454 periphyton algal component while is promoted when the heterotrophic O_2 respiration reduces the
455 volume of the oxic layer (Eriksson and Weisner, 1996; Venterink et al., 2003).
456 Although the relevance of biofilms on aquatic vegetation in contributing to N retention is widely
457 mentioned, the comparison of the obtained rates is limited to a few studies that have measured
458 specifically the contribution of this compartment. Denitrification rates measured on dead stems of
459 *P. australis* were in the upper range of values reported in the literature for a variety of epiphyton
460 and epilithon communities and in the most of the cases measured at higher temperatures than in the
461 present experiment (Table 4). Rates measured in the light were generally lower than those in the
462 dark, but on average higher than those previously measured in light, probably due to the
463 establishment of a heterotrophic-dominated biofilm (low chlorophyll-*a* content), where the
464 inhibitory effect of photosynthesis on denitrification is smaller. This explanation agrees with the
465 typical winter condition of the biofilms, when photosynthesis is at the lowest values and
466 heterotrophic metabolism dominates.
467 Our denitrification rates were on average distinctly higher than those measured by Toet and
468 collaborators (2003) on senescent *Phragmites* stems in a surface-flow wetland at similar winter
469 temperature (12°C) but at higher NO_3^- availability. However, comparisons with values recorded in
470 the literature need to be considered with caution because the body of denitrification rate
471 measurements in biofilms is almost totally dominated by the use of the acetylene inhibition-based
472 methods that have been criticized for underestimating the process (Fulweiler et al., 2015). The
473 underestimation is due to both the incomplete blockage of N_2O reduction to N_2, and more seriously,
474 to inhibition of nitrification that eliminates a possible substrate for denitrification (Groffman et al.,
475 2006: Fulweiler et al., 2015). Moreover, in several cases, only potential denitrification rates were
476 determined, under unlimited or optimal conditions of NO_3^- and organic carbon availability, and as
477 such not reflecting the *in situ* rates. The representativeness of denitrification rates presented here

478 and measured in intact sediments is proved by the simultaneous determination of N_2 production and
479 NO_3^- consumption. The two methods are robust, completely independent and thus the results are
480 representative of the actual ditch N removal capacity under in field conditions.
481
482 *4.3 Implications for vegetation management in drainage networks*
483 Agricultural landscapes have a buffering capacity towards NO_3^- pollution thanks to the mitigation
484 potential exerted by the extended networks of drainage and irrigation ditches, especially if in-stream
485 and riparian vegetation is maintained (Castaldelli et al., 2015; Romero et al., 2016; Speir et al.,
486 2017). An increasing number of studies have investigated the role of macrophytes in N dynamics
487 during the vegetative phase but their role during the cold season remains understudied.
488 Harvesting of above-ground biomass has been proposed by many authors as an effective practice to
489 control NO_3^- pollution and improve water quality of eutrophic ecosystems (Hansson and
490 Fredriksson, 2004; Quilliam et al., 2015). The best period for mowing generally coincides with the
491 peak in biomass and nutrient retention, resulting in the greatest nutrient removal from the system
492 (Ruiz and Velasco, 2010; Wang et al., 2014).
493 The yearly maintenance operations of the canal networks, such as the removal of senescent
494 emergent vegetation, as well as other cleaning and purging actions are performed at the end of
495 summer, before the period of intense rainfall. These are standard management practices aimed at
496 maintaining the hydraulic efficiency, since an extensive vegetation growth may hamper water
497 discharge, increase water level and hence flood risk. It follows that there is agreement between
498 hydraulic maintenance operations and the belief that vegetation removal is useful for reducing
499 nutrient loads. In the light of the present results and others obtained in the same *P. australis* stand,
500 this intuitive practice is disproved. First of all, N sequestration in plant biomass is a small fraction
501 of the total N abatement in vegetated canals while the most part of it is due to the complex
502 synergistic action of macrophytes and bacterial communities, mostly via denitrification (Pierobon et
503 al., 2013; Castaldelli et al., 2015). In addition, denitrification performed by biofilms on senescent

stems proceeds beyond the growing season throughout the cold months and maintains the depuration capacity of drainage canals when high NO_3^- loads may be leached from agricultural fields.

Considering the typical features of ditches in the investigated area (depth 30-40 cm, water velocity 3-6 cm s^{-1}, discharge 20-100 l s^{-1}, NO_3^- concentration 50-100 µM) and the NO_3^- removal rates measured in the present study, we conclude that denitrification capacity, performed by biofilms on *P. australis* senescent stems, may give a reduction per linear kilometer up to 25% of the incoming NO_3^- load. Therefore, a more conservative management of vegetation, with the postponement of mowing to the end of winter, just before the start of the new growing season (i.e. the emergence of new shoots at the beginning of spring), would promote a higher N removal throughout the year. Of course, this management choice must be accompanied by hydraulic evaluation and preferentially foreseen for canals where sections can be enlarged, in proportion to the increase in hydraulic impedance, due to the presence of vegetation.

Acknowledgments

This work was financially supported by the PRIN 2015 Project NOACQUA (risposte di comuNità e processi ecOsistemici in corsi d'ACQUA soggetti a intermittenza idrologica) and by the Emilia-Romagna Region within the POR FESR 2007-2013 Program for the development of the regional High Technology Network. It was also supported by the Po Delta Regional Park of the Emilia-Romagna within a long-term research collaboration for the definition of management protocols for the control of eutrophication in the Po River delta.

References

Allen, R.G., Pereira, L.S., Raes, D., Smith, M. (1998). Crop evapotranspiration-Guidelines for computing crop water requirements-FAO Irrigation and drainage paper 56. FAO, Rome, 300(9), D05109.

Armstrong, F.A.J., Stearns, C.R., Strickland, J.D.H. (1967). The measurement of upwelling and subsequent biological process by means of the Technicon Autoanalyzer® and associated equipment. Deep Sea Research and Oceanographic, 14(3), 381-389

Arnon, S., Peterson, C.G., Gray, K.A., Packman, A.I. (2007a). Influence of flow conditions and system geometry on nitrate use by benthic biofilms: implications for nutrient mitigation. Environmental Science & Technology, 41(23), 8142-8148.

Arnon, S., Gray, K.A., Packman, A.I. (2007b). Biophysicochemical process coupling controls nitrogen use by benthic biofilms. Limnology and Oceanography, 52(4), 1665-1671.

Baldwin, D.S., Mitchell, A.M., Rees, G.N., Watson, G.O., Williams, J.L. (2006). Nitrogen processing by biofilms along a lowland river continuum. River Research and Applications, 22(3), 319-326.

Bastviken, S.K., Eriksson, P.G., Martins, I., Neto, J.M., Leonardson, L., Tonderski, K. (2003). Potential nitrification and denitrification on different surfaces in a constructed treatment wetland. Journal of Environmental Quality, 32(6), 2414-2420.

Bastviken, S.K., Eriksson, P.G., Premrov, A., Tonderski, K. (2005). Potential denitrification in wetland sediments with different plant species detritus. Ecological Engineering, 25(2), 183-190.

Castaldelli, G., Soana, E., Racchetti, E., Vincenzi, F., Fano, E.A., Bartoli, M. (2015). Vegetated canals mitigate nitrogen surplus in agricultural watersheds. Agriculture, Ecosystems & Environment, 212: 253-262.

548 Christensen, P.B., Nielsen, L.P., Sørensen, J., Revsbech, N.P. (1990). Denitrification in nitrate-rich
549 streams: Diurnal and seasonal variation related to benthic oxygen metabolism. Limnology and
550 Oceanography, 35(3), 640-651.

551 Cole, J.J., Caraco, N.F. (1998). Atmospheric exchange of carbon dioxide in a low wind oligotrophic
552 lake measured by the addition of SF6. Limnology and Oceanography, 43(4): 647-656.

553 Cox, B.A. (2003). A review of dissolved oxygen modelling techniques for lowland rivers. Science
554 of the Total Environment, 314, 303-334.

555 Dalsgaard, T., Nielsen, L.P., Brotas, V., Viaroli, P., Underwood, G.J.C., Nedwell, D.B., Sundbäck,
556 K., Rysgaard, S., Miles, A., Bartoli, M., Dong, L., Thornton, D.C.O., Ottosen, L.D.M., Castaldelli,
557 G., Risgaard-Petersen, N. (2000). Protocol Handbook for NICE-Nitrogen Cycling in Estuaries: A
558 Project Under the EU Research Programme. Marine Science and Technology (MAST III). National
559 Environmental Research Institute, Silkeborg, Denmark, 62 pp.

560 Eloubaldy, A.F. (1969) Wind waves and the reaeration coefficient in open channel flow. Ph.D.
561 Thesis, Colorado State University. Fort Collins, Colorado.

562 Eriksson, P.G. (2001). Interaction effects of flow velocity and oxygen metabolism on nitrification
563 and denitrification in biofilms on submersed macrophytes. Biogeochemistry, 55(1), 29-44.

564 Eriksson, P.G., Weisner, S.E.B. (1996). Functional differences in epiphytic microbial communities
565 in nutrient-rich freshwater ecosystems: an assay of denitrifying capacity. Freshwater Biology, 36(3),
566 555-562.

567 Eriksson, P.G., Weisner, S.E.B. (1997). Nitrogen removal in a wastewater reservoir: the importance
568 of denitrification by epiphytic biofilms on submersed vegetation. Journal of Environmental Quality,
569 26(3), 905-910.

570 Eriksson, P.G., Weisner, S.E.B. (1999). An experimental study on effects of submersed
571 macrophytes on nitrification and denitrification in ammonium-rich aquatic systems. Limnology and
572 Oceanography, 44(8), 1993-1999.

573 Faulwetter, J.L., Gagnon, V., Sundberg, C., Chazarenc, F., Burr, M.D., Brisson, J., Camper, A.K.,
574 Stein, O.R. (2009). Microbial processes influencing performance of treatment wetlands: a review.
575 Ecological Eengineering, 35(6), 987-1004.

576 Fulweiler, R.W., Heiss, E.M., Rogener, M.K., Newell, S.E., LeCleir, G.R., Kortebein, S.M.,
577 Wilhelm, S.W. (2015). Examining the impact of acetylene on N-fixation and the active sediment
578 microbial community. Frontiers in microbiology, 6:418.

579 Genereux D.P., Hemond H.F. (1992). Determination of gas exchange rate constant for a small
580 stream on Walker Branch watershed, Tennessee. Water Resources Research, 28(9), 2365-2374.

581 Groffman, P.M., Altabet, M.A., Böhlke, J.K., Butterbach-Bahl, K., David, M.B., Firestone, M.K.,
582 Giblin, A.E., Kana, T.M., Nielsen, L.P., Voytek, M.A. (2006). Methods for measuring
583 denitrification: diverse approaches to a difficult problem. Ecological Applications, 16(6), 2091-
584 2122.

585 Hansson, P.A., Fredriksson, H. (2004). Use of summer harvested common reed (*Phragmites*
586 *australis*) as nutrient source for organic crop production in Sweden. Agriculture, ecosystems &
587 environment, 102(3), 365-375.

588 Isaacs W.P., Chulavachana, P., Bogart, R. (1969). An experimental study of the effect of channel
589 surface roughness on the reaeration rate coefficient. Proceedings of the 24th Industrial Waste
590 Conference, Purdue University. p. 1464-1476

591 Isaacs, W.P., Gaudy, A.F. (1968). Atmospheric oxygenation in a simulated stream. Journal of the
592 Sanitary Engineering Division, 94(2), 319-314.

593 Jacobs, A.E., Harrison, J.A. (2014). Effects of floating vegetation on denitrification, nitrogen
594 retention, and greenhouse gas production in wetland microcosms. Biogeochemistry, 119(1-3), 51-
595 66.

596 Jähne, B., Münnich, K.O., Bösinger, R., Dutzi, A., Huber, W., Libner, P. (1987). On parameters
597 influencing air-water exchange. Journal of Geophysical Research: Oceans, 92(C2), 1937-1949.

598 Kana, T.M., Darkangelo, C., Hunt, M.D., Oldham, J.B., Bennett, G.E., Cornwell, J.C. (1994).
599 Membrane inlet mass spectrometer for rapid high-precision determination of N_2, O_2, and Ar in
600 environmental water samples. Analytical Chemistry, 66(23), 4166-4170.

601 Kiss, M.K., Lakatos, G., Borics, G., Gidó, Z., Deák, C. (2003). Littoral macrophyte–periphyton
602 complexes in two Hungarian shallow waters. Hydrobiologia, 506(1), 541-548.

603 Kjellin, J., Hallin, S., Wörman, A. (2007). Spatial variations in denitrification activity in wetland
604 sediments explained by hydrology and denitrifying community structure. Water Research, 41(20),
605 4710-4720.

606 Kreiling, R.M., Richardson, W.B., Cavanaugh, J.C., Bartsch, L.A. (2011). Summer nitrate uptake
607 and denitrification in an upper Mississippi River backwater lake: the role of rooted aquatic
608 vegetation. Biogeochemistry, 104(1-3), 309-324.

609 Laursen A.E., Seitzinger S.P. (2002). Measurement of denitrification in rivers: an integrated, whole
610 reach approach. Hydrobiologia, 485, 67-81.

611 Lorenzen, C.J. (1967). Determination of chlorophyll and phaeo-pigments: spectrophotometric
612 equations. Limnology and Oceanography, 12(2), 343-346.

613 Messer, T.L., Burchell, M.R., Böhlke, J. K., Tobias, C.R. (2017). Tracking the fate of nitrate
614 through pulse-flow wetlands: A mesocosm scale ^{15}N enrichment tracer study. Ecological
615 Engineering, 106, 597-608.

616 Negulescu, M, Rojanski V. (1969). Recent research to determine reaeration coefficient. Water
617 Research, 3(3), 189-202.

618 O'Connor, B.L., Hondzo, M. (2007). Enhancement and inhibition of denitrification by fluid-flow
619 and dissolved oxygen flux to stream sediments. Environmental Science & Technology, 42(1), 119-
620 125.

621 Padden, T.J., Gloyna, E.F. (1972). Simulation of stream processes in a model river. Technical
622 Report No. 2 (EHE-70-23, CRWR-72). Austin, Texas: Texas University, Center for Reasearch in
623 Water Resources.

624 Palumbo, J.E., Brown, L.C. (2013). Assessing the performance of reaeration prediction equations.
625 Journal of Environmental Engineering, 140(3), 04013013.

626 Pang, S., Zhang, S., Lv, X., Han, B., Liu, K., Qiu, C., Wang, C., Wang, P., Toland, H., He, Z.
627 (2016). Characterization of bacterial community in biofilm and sediments of wetlands dominated by
628 aquatic macrophytes. Ecological Engineering, 97, 242-250.

629 Pierobon, E., Castaldelli, G., Mantovani, S., Vincenzi, F., Fano, E.A. (2013). Nitrogen removal in
630 vegetated and unvegetated drainage ditches impacted by diffuse and point sources of pollution.
631 CLEAN-Soil Air Water, 41, 24-31.

632 Quilliam, R.S., van Niekerk, M.A., Chadwick, D.R., Cross, P., Hanley, N., Jones, D.L., A.J.A.,
633 Vinten, N., Willby, D.M. Oliver (2015). Can macrophyte harvesting from eutrophic water close the
634 loop on nutrient loss from agricultural land? Journal of Environmental Management, 152, 210-217.

635 Rehman, F., Pervez, A., Khattak, B. N., Ahmad, R. (2017). Constructed wetlands: Perspectives of
636 the oxygen released in the rhizosphere of macrophytes. CLEAN-Soil, Air, Water, 45 (1) 1600054

637 Revsbech, N.P., Jacobsen, J.P., Nielsen, L.P. (2005). Nitrogen transformations in
638 microenvironments of river beds and riparian zones. Ecological Engineering, 24(5), 447-455.

639 Roeselers, G., Van Loosdrecht, M.C.M., Muyzer, G. (2008). Phototrophic biofilms and their
640 potential applications. Journal of Applied Phycology, 20(3), 227-235.

641 Romero, E., Garnier, J., Billen, G., Peters, F., Lassaletta, L., 2016. Water management practices
642 exacerbate nitrogen retention in Mediterranean catchments. Science of the Total Environment, 573,
643 420-432.

644 Ruiz, M., Velasco, J. (2010). Nutrient bioaccumulation in *Phragmites australis*: management tool
645 for reduction of pollution in the Mar Menor. Water, air, and soil pollution, 205(1-4), 173.

646 Schaller, J.L., Royer, T.V., David, M.B., Tank, J.L. (2004). Denitrification associated with plants
647 and sediments in an agricultural stream. Journal of the North American Benthological Society,
648 23(4), 667-676.

649 Shen, L.D., Zheng, P.H., Ma, S.J. (2016). Nitrogen loss through anaerobic ammonium oxidation in
650 agricultural drainage ditches. Biology and Fertility of Soils, 52(2), 127-136.

651 Silvester, N.R., Sleigh, M.A. (1985). The forces on microorganisms at surfaces in flowing water.
652 Freshwater Biology, 15(4), 433-448.

653 Sirivedhin, T., Gray, K.A. (2006). Factors affecting denitrification rates in experimental wetlands:
654 field and laboratory studies. Ecological Engineering, 26(2), 167-181.

655 Soana, E., Balestrini, R., Vincenzi, F., Bartoli, M., Castaldelli, G. (2017). Mitigation of nitrogen
656 pollution in vegetated ditches fed by nitrate-rich spring waters. Agriculture Ecosystem &
657 Environment. 243, 74-82.

658 Sørensen, J., Jørgensen, T., Brandt, S. (1988). Denitrification in stream epilithon: seasonal variation
659 in Gelbaek and Rabis Baek, Denmark. FEMS Microbiology Letters, 53(6), 345-353.

660 Speir, S.L., Taylor, J.M., Scott, J.T. (2017). Seasonal differences in relationships between nitrate
661 concentration and denitrification rates in ditch sediments vegetated with rice cutgrass. Journal of
662 Environmental Quality, 46(6), 1500-1509.

663 Srivastava, J.K., Chandra, H., Kalra, S.J., Mishra, P., Khan, H., Yadav, P. (2017). Plant–microbe
664 interaction in aquatic system and their role in the management of water quality: a review. Applied
665 Water Science, 7(3), 1079-1090.

666 Taylor, J.M., Moore, M.T., Scott, J.T., 2015. Contrasting nutrient mitigation and denitrification
667 potential of agricultural drainage environments with different emergent aquatic macrophytes.
668 Journal of Environmental Quality 44(4), 1304-1314.

669 Teissier, S., Torre, M. (2002). Simultaneous assessment of nitrification and denitrification on
670 freshwater epilithic biofilms by acetylene block method. Water Research, 36(15), 3803-3811.

671 Toet, S., Huibers, L.H., Van Logtestijn, R.S., Verhoeven, J.T. (2003). Denitrification in the
672 periphyton associated with plant shoots and in the sediment of a wetland system supplied with
673 sewage treatment plant effluent. Hydrobiologia, 501(1), 29-44.

674 Venterink, H. O., Hummelink, E., Van den Hoorn, M.W. (2003). Denitrification potential of a river
675 floodplain during flooding with nitrate-rich water: grasslands versus reedbeds. Biogeochemistry,
676 65(2), 233-244.

677 Vila-Costa, M., Pulido, C., Chappuis, E., Calvino, A., Casamayor, E. O., Gacia, E. (2016).
678 Macrophyte landscape modulates lake ecosystem-level nitrogen losses through tightly coupled
679 plant-microbe interactions. Limnology and Oceanography, 61(1), 78-88.

680 Wang, C.Y., Sample, D.J., Bell, C. (2014). Vegetation effects on floating treatment wetland nutrient
681 removal and harvesting strategies in urban stormwater ponds. Science of the Total Environment,
682 499, 384-393.

683 Wanninkhof, R. (1992). Relationship between gas exchange and wind speed over the ocean. Journal
684 of Geophysical Resource, 97: 7373-7381.

685 Weisner, S.E.B., Eriksson, P.G., Granéli, W., Leonardson, L. (1994). Influence of macrophytes on
686 nitrate. Ambio, 23(6): 363-366.

687 Weiss, R.F. (1970). The solubility of nitrogen, oxygen and argon in water and seawater. Deep Sea
688 Research and Oceanographic Abstracts 17(4), 721-735.

689 Wetzel, R.G. (Ed.). (1983). Periphyton of Freshwater Ecosystems: Proceedings of the First
690 International Workshop on Periphyton of Freshwater Ecosystems Held in Växjö, Sweden, 14–17
691 September 1982 (Vol. 17). Springer Science & Business Media.

692 Yamamoto, M., Murai, H., Takeda, A., Okunishi, S., Morisaki, H. (2005). Bacterial flora of the
693 biofilm formed on the submerged surface of the reed *Phragmites australis*. Microbes and
694 Eenvironments, 20(1), 14-24.

695 Zhang, S., Pang, S., Wang, P., Wang, C., Guo, C., Addo, F.G., Li, Y. (2016). Responses of bacterial
696 community structure and denitrifying bacteria in biofilm to submerged macrophytes and nitrate.
697 Scientific Reports, 6, 36178.

698 Zhou, S., Borjigin, S., Riya, S., Terada, A., Hosomi, M. (2014). The relationship between anammox
699 and denitrification in the sediment of an inland river. Science of the Total Environment, 490, 1029-
700 1036.

701 Wetzel, R. G., Søndergaard, M. (1998). Role of submerged macrophytes for the microbial
702 community and dynamics of dissolved organic carbon in aquatic ecosystems. In The structuring role
703 of submerged macrophytes in lakes (pp. 133-148). Springer New York.

704

705 **Table 1.** Water column features at the beginning of each incubation. Average values±standard
706 deviation of mesocosms with bare sediment and of mesocosms with biofilms on dead stems (*n*=6)
707 are reported. Ranges of gas transfer velocity (k600) for each velocity level were calculated as
708 described in the Material and Methods section.

709

Velocity (cm s^{-1})	**k600** (cm h^{-1})	**Dark/Light**	**T** (°C)	**Conductivity** (µS cm^{-1})	**NO_3^-** (µM)
0	0.45	Dark	10.40±0.82	578±57	98±1
		Light	10.22±0.72	588±63	95±1
1.5	0.45-0.99	Dark	10.27±0.25	585±74	100±2
		Light	10.47±0.30	589±76	100±3
3	0.88-1.69	Dark	11.59±0.43	614±77	97±3
		Light	11.35±0.31	619±80	97±3
6	1.81-3.00	Dark	11.03±0.31	567±70	103±1
		Light	10.83±0.09	586±74	102±2

710

711 **Table 2.** Results of the two–way ANOVA performed to test the effect of factors *velocity* and *light*
712 *(light/dark)* on NO_3^- removal and N_2 production rates measured in bare sediment mesocosms, in
713 mesocosms with biofilms on dead stems, and corrected rates ascribed to biofilms alone.

Variable	Factor	df	Sediment		Sediment + dead stems with biofilms		Only biofilms	
			F	*p*	*F*	*p*	*F*	*p*
NO_3^- removal	Velocity	3	3.211	0.051	4.848	**0.014**	7.324	**0.003**
	Light/dark	1	11.880	**0.003**	7.925	**0.012**	3.715	0.072
	Velocity x Light/Dark	3	0.553	0.653	0.978	0.428	1.582	0.233
N_2 production	Velocity	3	1.631	0.222	9.582	**<0.001**	8.260	**0.002**
	Light/dark	1	0.167	0.688	7.280	**0.016**	3.952	0.064
	Velocity x Light/Dark	3	0.918	0.454	0.565	0.646	0.243	0.865

714

715 Degrees of freedom (df), F-test value (*F*) and significance level (*p*) are reported. Significant
716 differences ($p<0.05$) are in bold.
717

718 **Table 3.** Results of the Holm-Sidak multiple comparison test performed on NO_3^- removal and N_2
719 production rates measured in mesocosms with biofilms on dead stems to identify significant
720 differences among velocity levels. Significant differences (p<0.05) are in bold.

721

Variable	Comparison	*p*
NO_3^- removal	6 cm s^{-1} vs 1.5 cm s^{-1}	**0.003**
	6 cm s^{-1} vs 0 cm s^{-1}	**0.009**
	6 cm s^{-1} vs 3 cm s^{-1}	**0.029**
	3 cm s^{-1} vs 1.5 cm s^{-1}	0.272
	3 cm s^{-1} vs 0 cm s^{-1}	0.562
	0 cm s^{-1} vs 1.5 cm s^{-1}	0.593
N_2 production	6 cm s^{-1} vs 1.5 cm s^{-1}	**<0.001**
	6 cm s^{-1} vs 0 cm s^{-1}	**0.002**
	6 cm s^{-1} vs 3 cm s^{-1}	**0.002**
	3 cm s^{-1} vs 1.5 cm s^{-1}	0.225
	3 cm s^{-1} vs 0 cm s^{-1}	0.871
	0 cm s^{-1} vs 1.5 cm s^{-1}	0.172

722

723 **Table 4.** Literature summary of denitrification rates measured in biofilms on aquatic vegetation and
724 other substrates.

Substrate	Site	T (°C)	NO_3^- (µM)	Chl-*a* (mg m^{-2})	Denitrification rate* (µmol N m^{-2} h^{-1})	Reference
Phragmites australis	Surface-flow wetland (The Netherlands)	8-17.5	70-570	<5-80	71-357	Toet et al., 2003
Phragmites australis	River Rhine (The Netherlands)	16	<215	-	4-143 (dark) up to 4 (light)	Venterink et al., 2003
Phragmites australis	Lake Biwa (Japan)	20	1000	-	100-480	Yamamoto et al., 2005
Elodea nuttallii	Surface-flow wetland (The Netherlands)	8-17.5	57-430	20-75	14-93	Toet et al., 2003
Potamogeton pectinatus	Shallow macrophye-dominated ponds (Sweden)	20	715	-	up to 15	Eriksson, 2001
Myriophyllum spicatum	Surface-flow wetland (Sweden)	20	1000	-	up to 450	Bastviken et al., 2003
Potamogeton spp., *Cladophora spp.*	Big Ditch (3rd-order tributary to the Sangamon River, USA)	7-28	2-1260	-	up to 20	Schaller et al., 2004
Pebbles	Garonne River (France)	Summer	285	243–379	0-580 (dark) 0-100 (light)	Teissier and Torre, 2002
Artificial substrates	Ovens River (Australia)	Late summer	100	0.1-1.6	up to 10	Baldwin et al., 2006
Phragmites australis	Drainage canal (Italy)	10-12	100	9-15	94-292 (dark) 63-231 (light)	This study

725 * Rates are reported per m^2 of colonised surface. For all references from the literature,
726 denitrification was measured by the acetylene block method, with the only exception of
727 Eriksson (2001) where $^{15}NO_3^-$ addition was used. Where not otherwise indicated, rates were
728 measured in dark conditions. N_2 fluxes obtained for biofilms alone in the present study are
729 reported for comparison.

Figure captions

Fig. 1. Scheme of the experimental mesocosms.

Fig. 2. Hourly rates of NO_3^- removal (average±standard deviation, *n*=3) and N_2 production (average±standard deviation, *n*=3) measured in bare sediment mesocosms and in mesocosms with biofilms on dead stems across the velocity range. Rates are expressed per m^2 of sediment in the mesocosm.

Fig. 3. NO_3^- removal and N_2 production rates ascribed to biofilms alone (average±standard deviation, *n*=3). Values are expressed per m^2 of colonised reed surface. Daily rates are calculated on the basis of a 11 h light/13 h dark cycle.

Fig. 4. Contribution of biofilm and sediment to overall NO_3^- removal and N_2 production (average±standard deviation, *n*=3) in a dead stand of *P. australis* across the velocity range. Rates are expressed per m^2 of sediment in the mesocosm. Daily rates are calculated on the basis of a 11 h light/13 h dark cycle.

Fig. 5. Correlation between daily rates of NO_3^- removal and N_2 production. Rates are expressed per m^2 of sediment in the mesocosm. Daily rates are calculated on the basis of a 11 h light/13 h dark cycle.

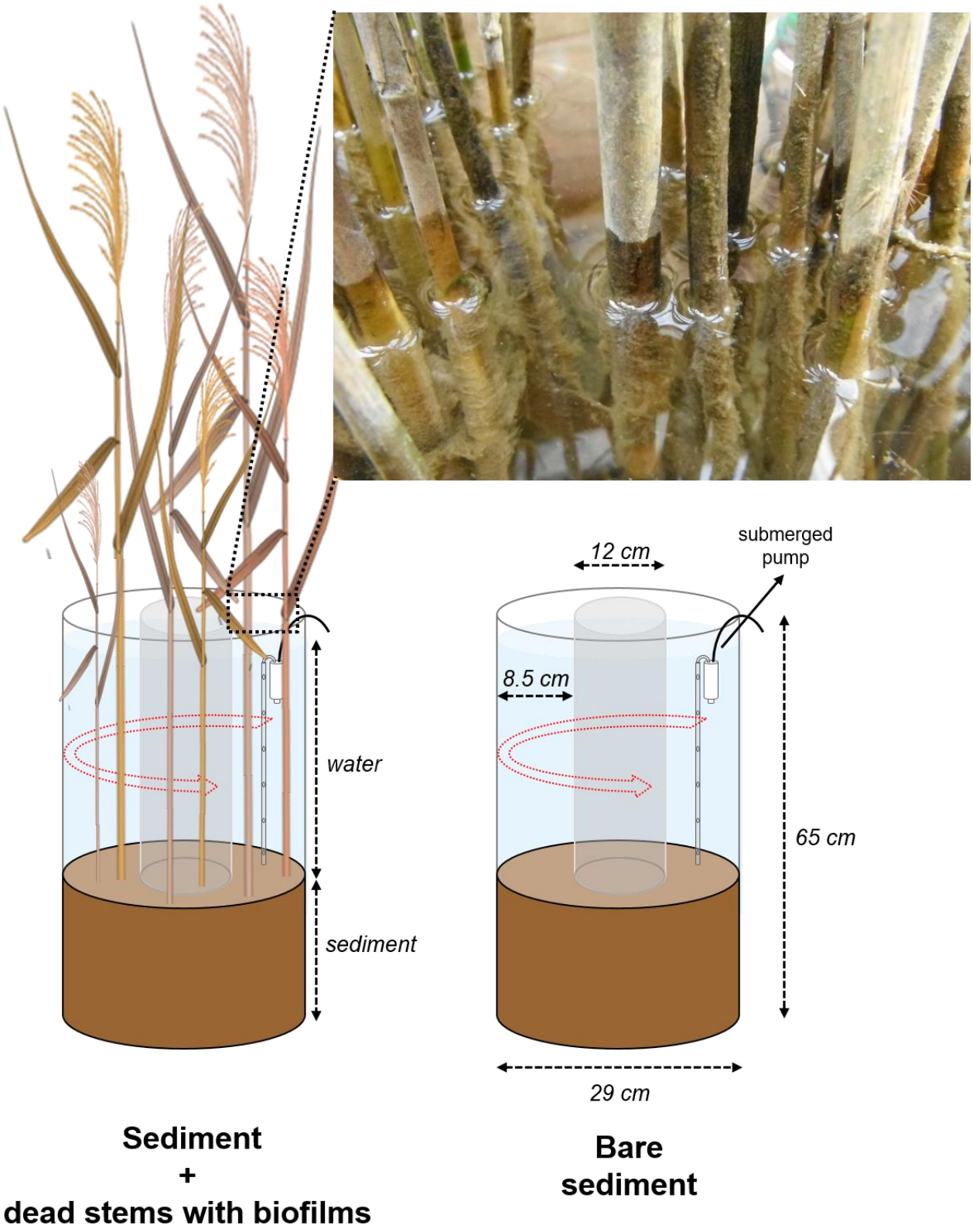
12 cm
submerged pump
8.5 cm
water
65 cm
sediment
29 cm
Sediment
+
dead stems with biofilms
Bare
sediment

749

750 Fig. 1

751 1

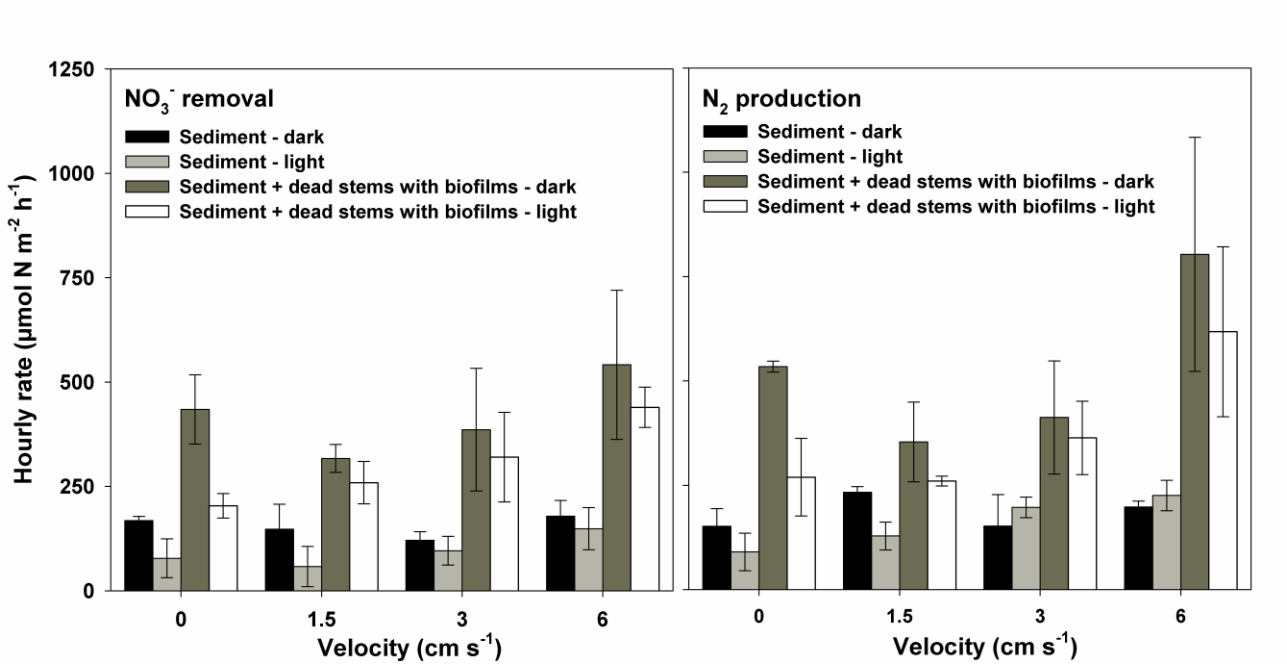

752

753 Fig. 2

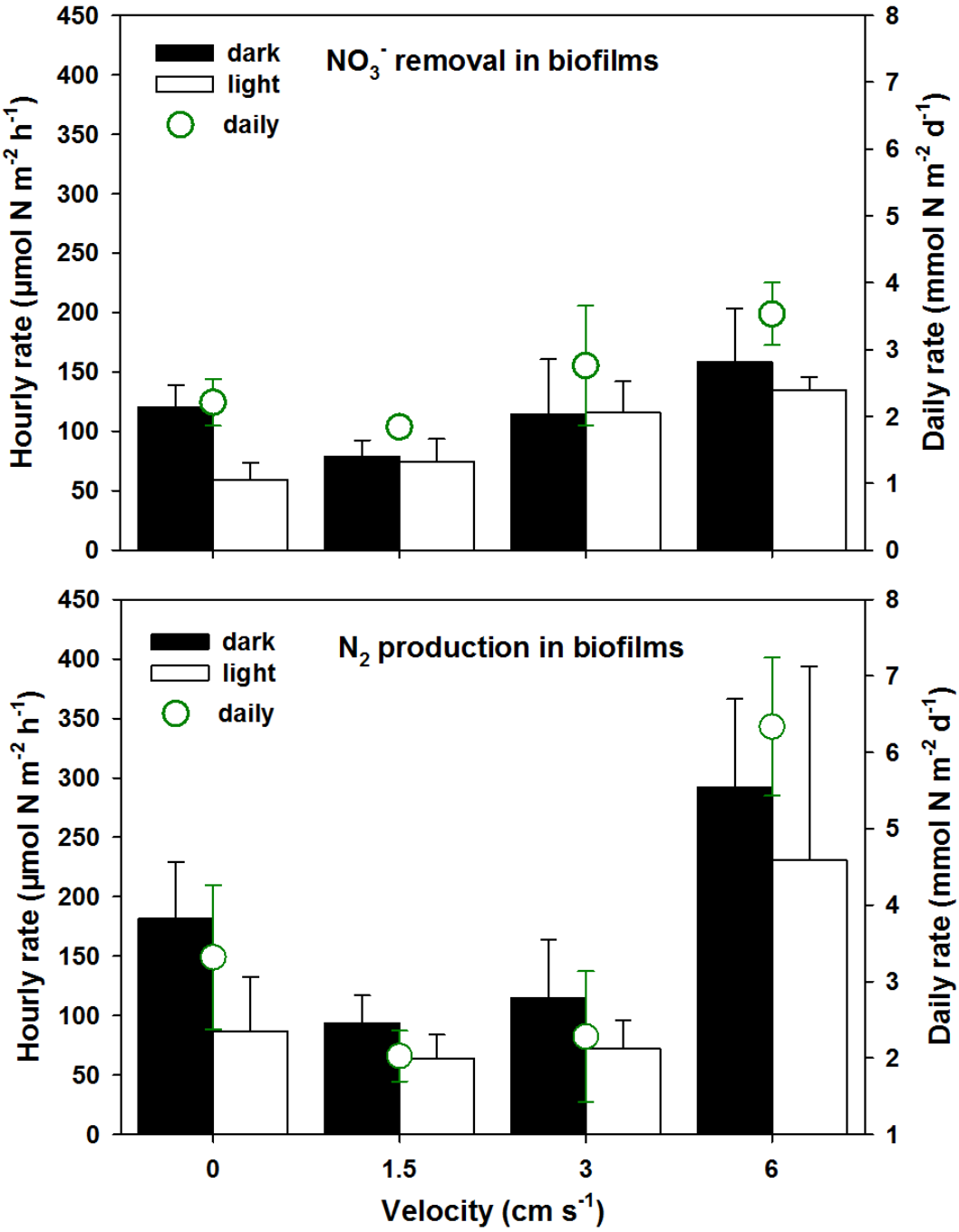
dark
light
daily
NO3- removal in biofilms
N2 production in biofilms
Hourly rate (µmol N m-2 h-1)
Daily rate (mmol N m-2 d-1)
Velocity (cm s-1)
0
1.5
3
6

754

755 Fig. 3

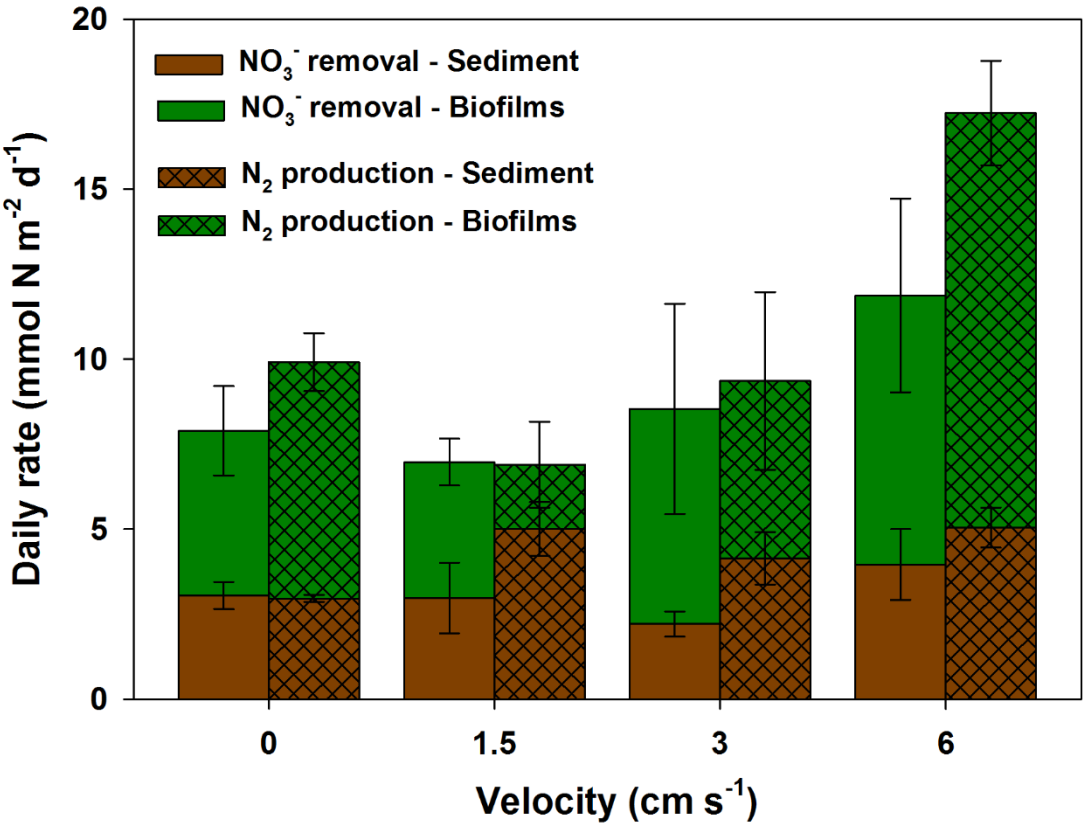
20
15
10
5
0
Daily rate (mmol N m-2 d-1)
NO3- removal - Sediment
NO3- removal - Biofilms
N2 production - Sediment
N2 production - Biofilms
0
1.5
3
6
Velocity (cm s-1)

756

757 Fig. 4

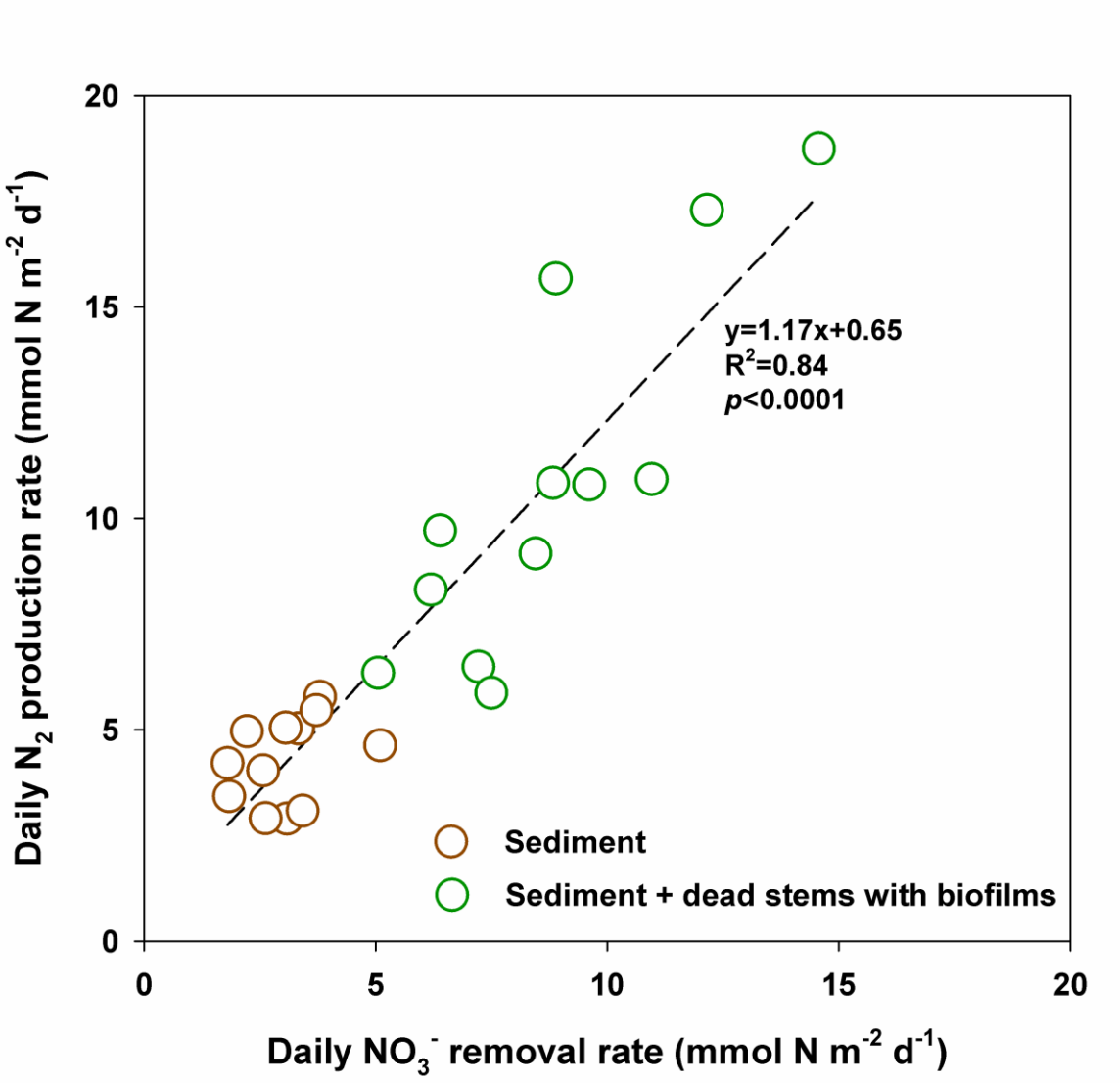
20
15
10
5
0
0
5
10
15
20
Daily N_2 production rate (mmol N m^{-2} d^{-1})
Daily NO_3^- removal rate (mmol N m^{-2} d^{-1})
y=1.17x+0.65
R^2=0.84
p<0.0001
Sediment
Sediment + dead stems with biofilms

758

759 Fig. 5